Intramolecular Effects and Relative Stabilities of Conformers of Gaseous Glycine

L. F. Pacios*

Departamento de Química y Bioquímica, E.T.S. Ingenieros de Montes, Universidad Politécnica de Madrid, E-28040 Madrid, Spain

O. Gálvez† and P. C. Gómez‡

Departamento de Química Física I, Facultad de Química, Universidad Complutense de Madrid, E-28040 Madrid, Spain

Received: November 9, 2000; In Final Form: February 28, 2001

Thirteen conformers of nonionized glycine identified previously in ab initio correlated calculations at the MP2/6-311++G** level of theory are investigated by means of the atoms in molecules (AIM) theory. The study focuses on properties directly derived from the electron density $\rho(\mathbf{r})$. The topological features of $\rho(\mathbf{r})$ are used to identify intramolecular hydrogen bonds in some structures. The intramolecular effects related with the stability of every conformer are explored by analyzing the potential energy contributions arising from the molecular fragments NH_2, CH_2, CO, and OH computed within the AIM framework. This study of intramolecular interactions using information provided by the $\rho(\mathbf{r})$ complements previous studies on glycine based on traditional empirical considerations and may be valuable for further studies on more complex amino acids.

Introduction

As the simplest amino acid ($NH_2-CHR-COOH$), glycine (R = H) has received special attention. Glycine crystallizes in the solid phase as a zwitterion $NH_3^+CH_2COO^-$. Neutron diffraction[1] and X-ray[2−5] structures have been reported, with the first X-ray work dating back to 1939.[2] The crystal structure has been characterized in X-ray studies at room temperature (combined with neutron diffraction),[3] at 120 K[4] and recently at 23 K.[5] In aqueous solution glycine presents the zwitterion form, but because the absorption due to water interferes with that of glycine itself, IR and Raman spectra are scarce[6] so that recent spectroscopic data on condensed phases refer to crystalline glycine.[7] On the theoretical side, zwitterionic glycine in the liquid phase has been the subject of ab initio calculations[8] and its vibrational spectrum in the aqueous medium recently studied.[9]

Much more evidence, both experimental[10−14] and theoretical,[15−23] exists for nonionized glycine in the gas phase. Glycine has three internal rotational degrees of freedom, ϕ, ψ, and θ, associated with bonds C−N, C−C, and C−O, respectively, seen in Figure 1. This leads to eight rotamers of C_s symmetry depicted in Figure 2 with roman numerals and the letter p to indicate planar heavy-atom arrangements (we follow the notation proposed by Császár[20]). Small torsional changes permit slight stabilizations leading to other minima in the potential energy surface (PES) displayed in Figure 2 with the letter n to denote nonplanar heavy-atom C_1 arrangements.

Two microwave studies of glycine were reported in 1978.[10,11a] Brown et al.[10] suggested that IIp should be the dominant species in the gas phase, whereas Suenram and Lovas[11a] proposed the mixture of Ip and IIp. These authors[11b] measured in 1980 the microwave spectrum of Ip, but due to uncertainties in the relative abundance of rotamers and the magnitude of dipole moments, it was not possible to determine the dominant species. Ijima et al.[12] reported in 1991 electron diffraction data and concluded that Ip is the most stable conformer, accounting for 76% in the gas phase; the remaning 24% should correspond to a mixture of IIp and IIIp.[12] Godfrey and Brown[13] used a free expansion supersonic jet microwave spectrometer to confirm the dominant mixture of Ip and IIp and suggested also the presence of IIIp.[13] Zheng et al.[14] observed the electron density of the highest occupied molecular orbital by multichannel electron momentum

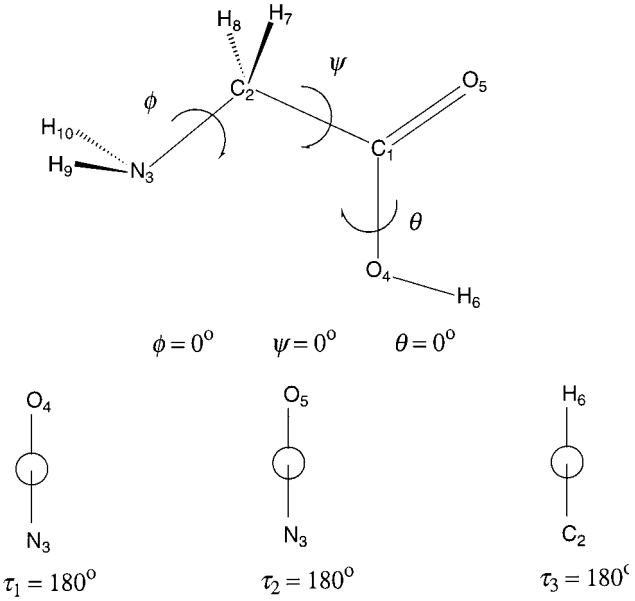

Figure 1. (Top) Atomic numbering scheme and internal rotational degrees of freedom ϕ, ψ, and θ for nonionized glycine. (Bottom) Newman projection of the dihedral angles τ_1 ($N_3C_2C_1O_4$), τ_2 ($N_3C_2C_1O_5$), and τ_3 ($C_2C_1O_4H_6$) used in ab initio calculations.

* Corresponding author (e-mail lpacios@montes.upm.es).
† E-mail ogalvez@eucmos.sim.ucm.es.
‡ E-mail pgc@eucmos.sim.ucm.es.

10.1021/jp004128e CCC: $20.00
Published on Web 05/04/2001

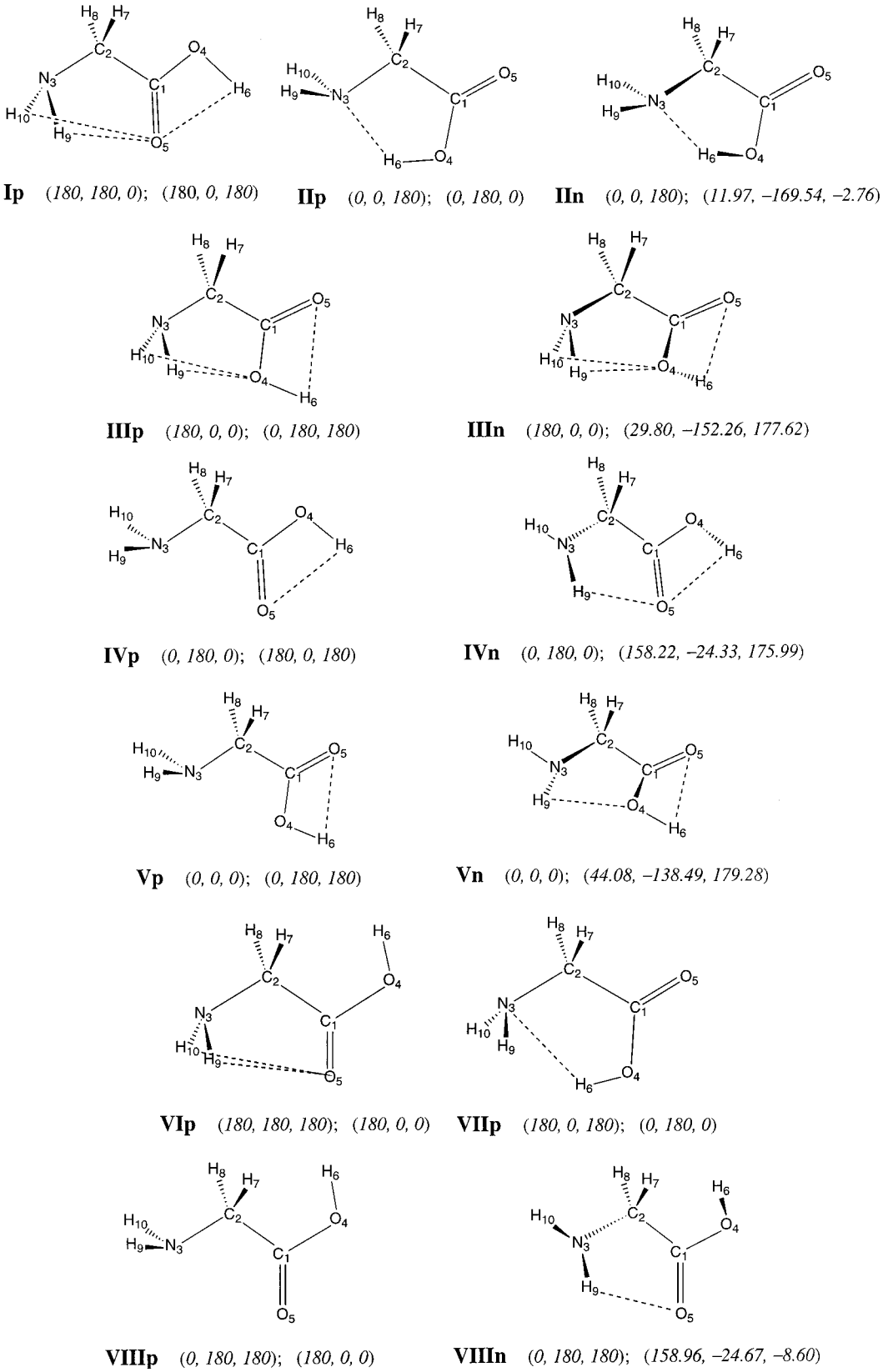

Figure 2. Conformers of glycine and sets of angles (ϕ, ψ, θ) and (τ_1, τ_2, τ_3) found in MP2/6-311++G** calculations.[20] Dashed lines represent assumed hydrogen bonds.

spectroscopy, finding an excellent agreement between their distribution and the theoretical distribution obtained with a weighted conformational average of the ab initio geometries of Császár[20] composed by Ip (55%), IIp (20%), IIIp (9%), IVn (13%), and Vn (3%).[14]

Pioneering ab initio work on glycine was reported in 1977 by Vishveshwara and Pople,[15] who computed HF/4-31G energies of rotamers generated at 60° intervals in ϕ, ψ, and θ angles. They identified Ip as the lowest lying conformer and IIp at 2.2 kcal/mol higher. Sellers and Schäfer[16] optimized the geometries of these two rotamers at the HF/4-21G level,[16a] obtaining a new estimate of 2.5 kcal/mol for their relative energy and suggesting

a third intermediate conformer IIIp at 1.9 kcal/mol above Ip.[16b] Using this information, Suenram and Lovas improved their previous microwave spectrum[11] and reported new results[16b] confirming Ip as the global minimum. Unfortunately, small changes in the basis sets used led to large fluctuations in the relative energies: at the end of the 1970s HF/DZ was the only ab initio level affordable to optimize geometries, but the resulting theoretical evidence was not conclusive enough to elucidate the PES of glycine.

Dykstra et al.[17] reported in 1981 the first correlated calculations and showed that electron correlation stabilizes IIp much more than Ip, decreasing their energy separation from 2.5 kcal/mol (HF value) to 1.0 kcal/mol.[17] In the 1990s, Jensen and Gordon[18] undertook an extensive study at the HF/6-31G* level and computed MP2 energies at the HF geometries. All of the conformers in Figure 2 except IIIn were identified, but their results suggested (misled by the small basis sets employed) that electron correlation had little effect on the relative stability. Ramek et al.[19] explored the influence of correlation to optimize geometries for Ip, IIp, and IIn at the MP2/6-311G** level and found significant changes that demonstrated the importance of using flexible basis sets. In 1992 Császár[20] reported MP2/6-311++G** geometries for all of the conformers, giving thus the first complete PES of glycine obtained with correlated calculations and extended basis sets. The information accumulated since the publication of the Császár work has confirmed the high reliability of his results. In a nearly simultaneous work apparently unaware of this study, Hu et al.[21] reported geometries at the CISD/DZP level for seven conformers with results very similar to Császár's. Shortly after publication of the Császár and Hu et al. papers, Barone et al.[22] reported LDA, BLYP, and B3LYP geometries and frequencies using DZ basis sets for eight rotamers and B3LYP/TZ2P results for Ip in a first attempt to explore the performance of DFT. They found that only the hybrid B3LYP method provides a reliability comparable to that of MP2, although their results could be hampered by the inadequacy of the basis set used. Nguyen et al.[23] have recently carried out DFT calculations with nonlocal functionals and larger basis sets, obtaining results in good agreement with the Császár data. All of these studies have thoroughly demonstrated the importance of electron correlation in ab initio calculations on glycine. Recent evidence points to the need of including correlation in any calculation involving amino acids.[24,25]

The relative energies of the rotamers have been rationalized in traditional terms used in chemistry in a qualitative manner. Thus, the competing effects of electron repulsions (particularly between N and O lone pairs) and steric strain on one side and intramolecular hydrogen bonding on the other side should account for that relative stability. The subtlety of these effects should be the main reason for the discrepancies found in theoretical studies depending on the different methodologies employed.

It is surprising that in all of the studies so far published on neutral glycine the information provided by the electron density $\rho(\mathbf{r})$ has been ignored. We feel that a further understanding of the interactions underlying the relative stabilities can be achieved with more rigorous tools applied to the electron distribution of the rotamers. Because the Császár results provide a reliable PES consisting of a large enough number of structures, glycine is a good candidate to explore the characterization of intramolecular effects in terms of information directly derived from $\rho(\mathbf{r})$. With this goal, we use in this work the atoms in molecules (AIM) theory,[26,27] which provides a rigorous procedure to partition a molecular system into its atomic fragments defined by the gradient vector field of $\rho(\mathbf{r})$. The AIM framework makes a bridge between the methods of quantum mechanics and traditional chemical concepts. The study here presented is thus intended not only to explore the conformational PES of glycine but to provide a way to analyze intramolecular interactions of further interest in amino acids.

TABLE 1: Relative Energies (ΔE) of Glycine Conformers Obtained with Different Correlated Calculations and MP2 Dipole Moments (μ)[a]

	ΔE					
conformer	MP2[b]	MP4[c]	MP∞[c]	BLYP[d]	ACM[d]	μ[e]
Ip	0.0	0.0	0.0	0.0	0.0	1.19
IIp	0.59	0.66	0.70	0.17	0.11	5.68
IIn	0.53	1.01	0.64	0.12	0.08	5.58
IIIp	1.59	1.54	1.52	1.44	1.56	1.77
IIIn	1.44	1.39	1.37	1.39	1.59	1.69
IVp	4.68	4.66	4.66	5.08	5.18	2.65
IVn	1.26	1.31	1.31	1.72	1.59	2.05
Vp	5.38	5.34	5.34	5.27	5.65	2.03
Vn	2.20	2.18	2.17	3.01	3.04	2.40
VIp	5.70	5.49	5.48	5.17	5.52	2.95
VIIp	6.97	6.92	6.90	5.82	6.20	4.08
VIIIp	11.19	10.92	10.90	10.84	11.83	5.51
VIIIn	7.09	6.92	6.91	6.96	7.13	4.30

[a] Energies in kcal/mol, dipole moments in debyes. [b] Full MP2/6-311++G** geometry optimization.[20] [c] Single-point MPn/6-311++G** calculations at the MP2/6-311++G** geometries.[20] [d] DFT/DZVP geometry optimizations.[23] [e] Computed at the MP2/6-311++G** geometries with the same basis set (this work).

The paper is organized as follows. The first section presents a brief account of the relative stabilities of glycine. The next section studies the intramolecular hydrogen bonding in the conformers. After reviewing the existing information that has been obtained from conventional arguments relying on interatomic distances and vibrational frequencies, we use the AIM theory to study the topology of $\rho(\mathbf{r})$ for characterizing the possible intramolecular H-bonds. The third section presents a study of the energetic contributions of the molecular groups to the different stabilities of the conformers. Finally, we present our main conclusions.

Relative Energies

The conformers of neutral glycine found by Császár at the MP2/6-311++G** level of theory identified with his notation[20] are displayed in Figure 2. Intramolecular hydrogen bonds supposedly existing in most conformers[20−23] are indicated in the form of dashed lines. Roman numerals I−VIII reflect the increasing relative energies of the heavy-atom planar C_s structures corresponding to the three rotational degrees of freedom (ϕ, ψ, and θ in Figure 1) labeled with the letter p. Small changes of the torsional angles (τ_1, τ_2, and τ_3 in Figure 1) yield the heavy-atom nonplanar C_1 arrangements identified with the letter n. Both sets of angles are given for every rotamer in Figure 2.

Table 1 lists relative energies ΔE computed with different methods. MP values are in close agreement except for the IIp−IIn difference, which changes from 0.06 kcal/mol in MP2 and MP∞ results to 0.35 kcal/mol in MP4. Császár also calculated single-point CCSD(T) energies for some conformers, obtaining ΔE values essentially identical to the MPn ones.[20] DFT results were obtained by Nguyen et al.[23] with a DZVP basis set, which is a standard 6-31G** set but optimized for DFT. A larger basis set termed TZVP (equivalent to 6-311G**) was explored, and negligible differences with respect to DZVP results were found

TABLE 2: Relative MP2/6-311++G Energies (ΔE), ZPE-Corrected Relative Energies (ΔE_0), and Total Free Energies at 473 K (ΔG_{473}) of Glycine[a]**

	MP2/6-311++G** [b]		
conformer	ΔE	ΔE_0	ΔG_{473}
Ip	0.0	0.0	0.0
IIn	0.53	0.90	1.62
IIp	0.59	0.78	3.36
IVn	1.26	1.27	1.80
IIIn	1.44		
IIIp	1.59	2.00	2.81
Vn	2.20	2.25	2.67
IVp	4.68		
Vp	5.38		
VIp	5.70	5.27	5.10
VIIp	6.97	6.43	6.49
VIIIn	7.09	6.72	7.19
VIIIp	11.19		

[a] Energies in kcal/mol. [b] ZPE corrections from ref 20 scaled by 0.97. ΔG_{473} values were determined from data in ref 23.

(however, we think that the use of diffuse functions could have modified the pattern of their data). The authors reported energies computed with two DFT approaches, BLYP and the adiabatic connection method (ACM) of Becke,[28] obtaining ΔE results consistently within 0.4 kcal/mol for both methods except in VIIIp, where they differ by 1 kcal/mol. Because the other DFT calculations reported[22] used DZP basis sets, the study by Császár may be considered to be the best post-HF treatment available.

With regard to MP2 dipole moments listed in Table 1, only three conformers display significantly larger values than the rest: IIp, IIn, and VIIIp. The last one is the most unstable rotamer, so its presence in gaseous glycine must be unnoticeable, but IIp and IIn are near the minimum and they must be easily observable in microwave spectra. The structure identified by all of the methods as the most stable conformer, Ip, happens to have the smallest dipole moment in all of the conformational PES.

Using MP2 vibrational frequencies (scaled by 0.97[20]), one obtains the zero-point energy (ZPE) corrected relative energies ΔE_0 in Table 2, where conformers have been arranged in ascending order of ΔE. The most noticeable effect of ZPE corrections is that ΔE for IIn and IIp increases by 0.37 and 0.19 kcal/mol, respectively, inverting their relative ordering. Nguyen et al.[23] derived from microwave intensities an expression for the conformational free energy difference at 473 K, also listed in Table 2. The scarce thermodynamical data available suggest that entropic contributions affect the relative stabilities of some rotamers, particularly IIn and IIp.[23] Only two experimental values of ΔG_{473} have been reported, 2.1[11b] and 1.7 kcal/mol,[12] both attributed to IIn.

Summarizing, the energetic picture of the conformational PES of neutral glycine is the following. There are three isomers, Ip, IIn, and IIp, within 1 kcal/mol, with Ip as the most stable structure. Four rotamers, IVn, IIIn, IIIp, and Vn, follow at relative energies between 1.3 and 2.2 kcal/mol above the minimum. There is a small gap, and then three conformers, IVp, Vp, and VIp, display ΔE values between 4.7 and 5.7 kcal/mol. Two structures, VIIp and VIIIn, follow at 7 kcal/mol, and finally VIIIp is the most unstable conformer by 11 kcal/mol. A somewhat striking result is that nonplanar C_1 isomers have lower energies than their planar C_s counterparts. This difference is very low in pairs II and III (0.1 and 0.2 kcal/mol, respectively), and much more marked in pairs IV (3.4 kcal/mol), V (3.2 kcal/mol), and VIII (4.1 kcal/mol).

Intramolecular Hydrogen Bonds

In all of the theoretical work hitherto done on nonionized glycine, it has been commonplace to attribute a dominant role to the intramolecular hydrogen bonds indicated by dashed lines in Figure 2 for understanding the relative stability of the conformers.[19−23] In the most complete study of Császár, intramolecular H-bonds of different strengths are identified on the basis of computed interatomic distances and vibrational frequencies. For instance, the existence of two equal N−H···O bonds in Ip and one O−H···N bond in IIp and IIn was suggested.[20] After examining a previous proposal by Barone et al.,[22] Hu et al.[21] suggested the following four types of hydrogen bonds (see Figure 2): (1) an $O_4-H_6\cdots O_5$ bond present in conformers Ip, IIIp, IIIn, IVp, IVn, Vp, and Vn; (2) an $O_4-H_6\cdots N_3$ bond in IIp, IIn, and VIIp; (3) a bifucarted arrangement between hydrogens in NH_2 and the O_5 atom of carbonyl in Ip and VIp; and (4) a similar arrangement but now with the O_4 atom of hydroxyl in IIIp and IIIn. This study was made in terms of interatomic distances and (in some selected cases) associated red shifts in the vibrational frequencies of stretching modes in NH and OH bonds upon formation of the H-bond. Types 1 and 2 were suggested as the most favorable bonds, and the five-membered ring type 2 was identified as the main factor in the stabilization of rotamers IIn and IIp (II and III in the notation used in ref 21). However, the authors did not discuss VIIp (VIII in their notation), which in principle can present a similar H-bond. Types 3 and 4 were considered to be less important than types 1 and 2 and, after the relative acceptor properties of oxygen atoms on carbonyl and hydroxyl were taken into account, type 4 was discarded as a true hydrogen bond.[21] Nguyen et al.[23] analyzed these same kinds of H-bonds (without using that classification) and studied the influence of basis sets and choice of DFT functionals on the interatomic distances involved. Their study on intramolecular hydrogen bonding relies exclusively on geometrical information, particularly NH···O and OH···N distances. Considering the especially short $O_4H_6\cdots N_3$ distance (∼1.9 Å) in conformers IIp and IIn, the authors concluded that the H-bond stabilizes especially these structures.[23]

In an attempt to characterize hydrogen bonds in a rigorous manner with the help of AIM theory, Popelier studied systems with well-known intermolecular H-bonds and proposed eight AIM-based criteria indicative of hydrogen bonding.[27,29] Four of them refer to topological properties of the electron density: (a) a bond critical point (BCP) with the consistent (3,−1) topology must exist; (b) the $\rho(\mathbf{r})$ at the BCP, ρ_b, must present a value within the range of 0.002−0.04 au; (c) the Laplacian of $\rho(\mathbf{r})$ at the BCP, $\nabla^2\rho_b$, must be positive, with values within the range of 0.015−0.15 au; and (d) hydrogen and acceptor atoms must mutually penetrate. The other four criteria refer to integrated properties of the H atom, which upon formation of an H-bond must exhibit (e) an increase of the net positive atomic charge (loss of charge), (f) energetic destabilization, (g) a decrease in the dipolar polarization, and (h) a decrease in the atomic volume. Popelier stated that possible H-bonds which fail one or more of these criteria cannot be designated real H-bonds and assumed that they are equally appliable to intermolecular and intramolecular hydrogen bonds.[27]

We have calculated the MP2/6-311++G** electron density $\rho(\mathbf{r})$ of all the conformers in Figure 2 at the optimized geometries of Császár with the GAUSSIAN98 package.[30] The topological analysis of $\rho(\mathbf{r})$ and the integration of atomic properties are carried out with the programs EXTREME, which locates and classifies the critical points, and PROAIM, which performs the numerical integration.[31,32] With the exception of

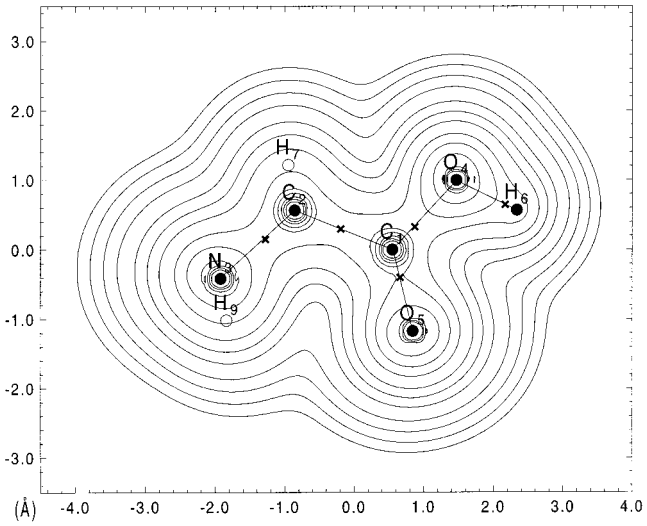

Figure 3. Contour map of the MP2/6-311++G** electron density for conformer Ip in the plane containing the heavy atoms and H_6. Open circles indicate the projection of H_7 and H_9 atoms. Crosses indicate bond critical points. The outermost contour is $\rho(\mathbf{r}) = 0.001$ au, and the remaining contours increase in the order 2×10^n, 4×10^n, and 8×10^n, with $n = -3, -2, -1$, and 0.

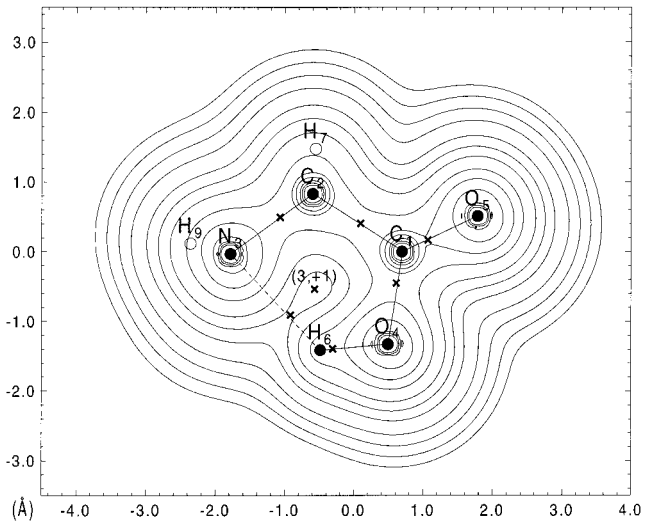

Figure 4. Contour map of the MP2/6-311++G** electron density for conformer IIp in the plane containing the heavy atoms and H_6. The projection of H_7 and H_9 atoms is shown as open circles. Crosses indicate critical points. See Figure 3 for contour values.

IIp, IIn, and VIIp, the only BCPs found in all cases are those located at the interatomic paths defined by covalent bonds as illustrated in Figure 3 where we have plotted $\rho(\mathbf{r})$ for the most stable conformer Ip in the plane containing the heavy atoms plus H_6. Figures 4, 5, and 6 display maps of $\rho(\mathbf{r})$ for conformers IIp, IIn, and VIIp, respectively. Only in these three rotamers have we found (i) an extra (3,−1) BCP in the path joining N_3 and H_6 atoms and (ii) a (3,+1) ring critical point (RCP) in the interior of the five-membered ring formed by N_3C_2, C_2C_1, C_1O_4, O_4H_6, and $H_6\cdots N_3$ paths. Conformers IIp (Figure 4) and IIn (Figure 5) display similar features and near values of the $N_3\cdots H_6$ distance (1.890 Å in IIp and 1.904 Å in IIn) and the distance between the $N_3\cdots H_6$ BCP and the RCP (0.533 Å in IIp and 0.494 Å in IIn). However, VIIp (Figure 6) displays a different situation. In fact, the close proximity between BCP and RCP (0.127 Å) reveals a clear instability in the associated bond.[27] Moreover, the N···H path is noticeably inwardly curved away from the perimeter of the ring, a property of electron-

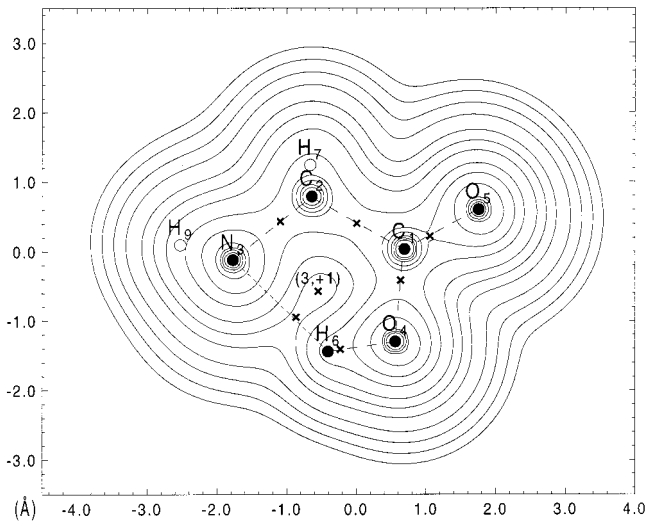

Figure 5. Contour map of the MP2/6-311++G** electron density for conformer IIn in a plane passing through heavy atoms and H_6. The projection of H_7 and H_9 atoms is shown as open circles. Crosses indicate critical points. See Figure 3 for contour values.

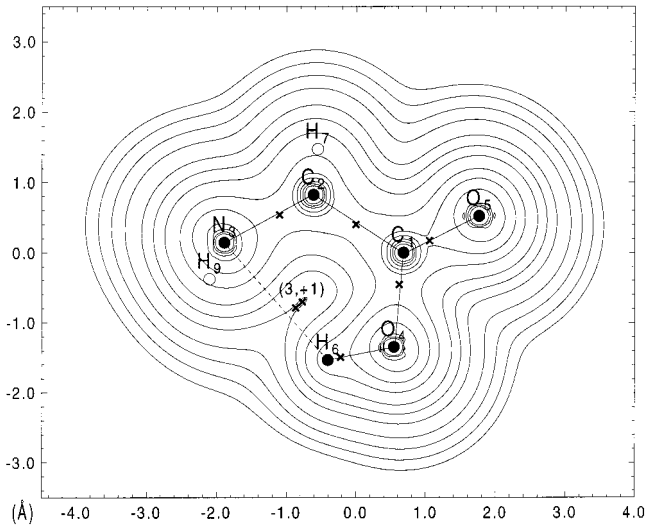

Figure 6. Contour map of the MP2/6-311++G** electron density for conformer VIIp in the plane containing the heavy atoms and H_6. The projection of H_7 and H_9 atoms is shown as open circles. Crosses indicate critical points. See Figure 3 for contour values.

deficient systems observed before.[26] Both features indicate that the $N_3\cdots H_6O_4$ hydrogen bond in VIIp is unstable, which is consistent with the $N_3\cdots H_6$ distance, 2.239 Å, much larger than that of IIp and IIn.

Table 3 lists values of the electron density and its Laplacian at the critical point, ρ_b and $\nabla^2\rho_b$, as well as bond ellipticities ϵ for conformers IIp, IIn, and VIIp. It must be recalled that the two negative eigenvalues λ_1 and λ_2 of the Hessian of the density in a (3,−1) BCP are used to define $\epsilon = [(\lambda_1/\lambda_2) - 1]$. The ellipticity is taken as a measure of the extent to which ρ is accumulated in the plane defined by the axes of curvature λ_1 and λ_2, both perpendicular to the bond path. ϵ has been related to the π character of a bond: it is nearly zero in single bonds and increases to 0.176 for the CC bond in benzene and to 0.298 in ethene.[26,27] The features of the BCPs in covalent bond paths for all of the conformers under study are found to be very similar and also agree with those of BCPs in experimental electron densities in other amino acids such as DL-histidine, DL-aspartic acid, or L-alanine.[25] Although distinct values of ϵ are shown in

TABLE 3: Critical Point Properties of the MP2/6-311++G Electron Density of Glycine Conformers IIp, IIn, and VIIp[a]**

path	ρ_b	$\nabla^2\rho_b$	ϵ
	IIp		
C_1-C_2	0.252	−0.611	0.103
C_2-N_3	0.259	−0.694	0.048
C_1-O_4	0.303	−0.374	0.023
C_1-O_5	0.412	−0.076	0.106
O_4-H_6	0.340	−2.395	0.016
$C_2-H_{7,8}$	0.278	−0.945	0.034
$N_3-H_{9,10}$	0.335	−1.591	0.047
$N_3\cdots H_6$	0.038	+0.109	0.114
(3,+1) RCP	0.029	+0.170	-
	IIn		
C_1-C_2	0.252	−0.614	0.101
C_2-N_3	0.260	−0.696	0.041
C_1-O_4	0.302	−0.377	0.022
C_1-O_5	0.413	−0.075	0.108
O_4-H_6	0.341	−2.406	0.016
C_2-H_7	0.278	−0.948	0.034
C_2-H_8	0.277	−0.943	0.031
N_3-H_9	0.335	−1.579	0.045
N_3-H_{10}	0.335	−1.591	0.046
$N_3\cdots H_6$	0.037	+0.108	0.126
(3,+1) RCP	0.029	+0.167	
	VIIp		
C_1-C_2	0.250	−0.601	0.106
C_2-N_3	0.266	−0.730	0.032
C_1-O_4	0.291	−0.361	0.041
C_1-O_5	0.415	−0.055	0.108
O_4-H_6	0.358	−2.510	0.018
$C_2-H_{7,8}$	0.279	−0.955	0.037
$N_3-H_{9,10}$	0.335	−1.579	0.061
$N_3\cdots H_6$	0.020	+0.072	1.973
(3,+1) RCP	0.020	+0.084	

[a] Except the (3,+1) ring CPs indicated, the rest are (3,−1) bond CPs. ρ_b and $\nabla^2\rho_b$ are the electron density and its Laplacian at the CP (both in atomic units). ϵ is the ellipticity.

Table 3 for C_1O_4 and C_1O_5 bonds, as expected from their different electron environment, the C_1O_4 bond has an ellipticity similar to that of hydroxyl, whereas ϵ for carbonyl C_1O_5 is nearly identical to C_1C_2 bond, which is more surprising. On the other hand, the large negative values of $\nabla^2\rho_b$ in OH and NH bonds indicative of concentration of charge are consistent with the close proximity to hydrogens of the BCPs in these bonds (see Figures 3−6), which explains the high values of these ρ_b, too.

The (3,−1) BCP in the $N_3\cdots H_6$ path and the (3,+1) RCP support the existence of intramolecular hydrogen bonds in IIp, IIn, and VIIp. However, the anomalous ellipticity of the BCP in VIIp, 1.973, a consequence of its close proximity to the RCP,[27] reveals the instability of this hydrogen bond as noted above. The BCPs in $N_3\cdots H_6$ paths shown in Table 3 meet criteria a−c. The prescription given by Popelier[27,29] to quantify the effect of criterion d consists of comparing the nonbonded radii (r^0) of both atoms with the corresponding bonded radii (r), so that the mutual penetration means that $r^0_H - r_H > 0$ and $r^0_B - r_B > 0$. Whereas r^0 is estimated as the distance from the nucleus to a given density contour (typically 0.001 au) in the H-bond direction, r is simply the distance from the nucleus to the BCP. This criterion is obviously fulfilled in intramolecular cases such as those displayed in Figures 4−6, where the outermost contour of ρ is just 0.001 au.

Table 4 lists the AIM integrated properties concerning criteria e−h for the H_6 atom in all of the conformers. Interatomic distances from H_6 to both oxygens in carboxyl are also given in this table. A check on the accuracy of the numerical integrations is provided by $L(\Omega)$, the integral of $\nabla^2\rho$ over the basin Ω of the atom: due to the boundary condition of zero flux to define Ω, it must be zero. Values of L in Table 4 are in the range of 5.1×10^{-4} to $2.5 \times 10^{-}$,[5] which is known to represent errors in the estimates of energies of $\sim 10^{-4}$ hartrees.[26] Because we are examining intramolecular hydrogen bonds, the change in the atomic properties described by criteria e−h cannot be evaluated with respect to the isolated monomers but to other conformers where similar H bonds are not possible. As for data in Table 4, the increase of atomic charge, energetic destabilization, decrease of dipolar polarization, and decrease of atomic volume in conformers IIp and IIn when compared to the rest of rotamers are evident. However, VIIp fails to meet criteria e−h, and therefore it cannot form a true intramolecular H-bond. In light of these criteria, the properties of the H-bond in IIp and IIn are nearly indistinguishable. Note how the hydroxyl bond length in these rotamers increases, as should be expected upon formation of the $N_3\cdots H_6O_4$ hydrogen bond according to traditional chemical criteria.

TABLE 4: Integrated Atomic Properties of the H_6 Atom and Interatomic Distances to Both Oxygens in the Carboxyl Group in Glycine Conformers[a]

conformer	$q(\Omega)$	$E(\Omega)$	$\mu(\Omega)$	$V(\Omega)$	$d(O_4H_6)$	$d(O_5H_6)$
Ip	0.599	−0.3571	0.162	21.81	0.968	2.294
IIp	0.618	−0.3449	0.140	15.57	0.981	2.978
IIn	0.614	−0.3450	0.141	15.94	0.980	2.979
IIIp	0.600	−0.3569	0.162	21.75	0.968	2.280
IIIn	0.600	−0.3567	0.162	21.74	0.968	2.283
IVp	0.597	−0.3588	0.164	21.93	0.967	2.291
IVn	0.600	−0.3569	0.162	21.75	0.968	2.291
Vp	0.594	−0.3604	0.165	22.00	0.968	2.263
Vn	0.601	−0.3561	0.161	21.69	0.968	2.290
VIp	0.581	−0.3720	0.168	22.38	0.964	3.006
VIIp	0.579	−0.3703	0.168	20.07	0.966	2.990
VIIIp	0.573	−0.3762	0.172	22.70	0.964	3.007
VIIIn	0.584	−0.3702	0.166	21.96	0.963	3.001

[a] $q(\Omega)$ is the atomic charge, $E(\Omega)$ the total energy, $\mu(\Omega)$ the dipolar polarization, and $V(\Omega)$ the atomic volume. All of these values are in atomic units. Interatomic $d(O-H_6)$ distances are in Å.

It has been customary in the bibliography to treat the interaction between H_6 and O_5 atoms in carboxyl as a true H-bond in all of the rotamers with $\theta = 0°$. Although on the grounds of Popelier's criteria no hydrogen bonds other than those identified in IIp and IIn exist, the properties in Table 4 reveal valuable information on the interactions involving the H_6 atom. Excluding the already analyzed rotamers IIp and IIn, atomic charges and total energies for H_6 can be collected into two groups. On the one hand, conformers with $\theta = 180°$ (VIp, VIIp, VIIIp, and VIIIn) display $q(\Omega)$ between 0.573 and 0.584 and $E(\Omega)$ between −0.3702 and −0.3762 au. On the other hand, conformers with $\theta = 0°$ exhibit increased charges between 0.594 and 0.601 and destabilized energies between −0.3561 and −0.3588 au. Dipolar polarizations are slightly larger in the first group, whereas atomic volumes show no clear separation. If one looks at the interatomic distances in Table 4, the second group of conformers happens to display a consistent O_4H_6 bond length of 0.968 Å, longer than the length in the first group, 0.964 Å. This lengthening should be the expected result if the hydroxyl were involved in the formation of a hydrogen bond, which indeed could be also supported by the changes shown by $q(\Omega)$ and $E(\Omega)$. However, according to Popelier's criteria no real intramolecular H-bond may be identified in conformers with $\theta = 0°$, although an interaction somewhat reminiscent of hydrogen bonding seems to exist between O_5 and H_6 in them.

To analyze the bifurcated arrangements involving amino supposedly forming H-bonds of types 3 and 4, we list in Table 5 the atomic properties of the H_9 atom (rotamers IIp, IIn, and

TABLE 5: Integrated Atomic Properties of the H_9 Atom and Interatomic Distances to Nitrogen and the Nearest Oxygen O_x, $x = 4$ or 5, in Some Glycine Conformers[a]

conformer	$q(\Omega)$	$E(\Omega)$	$\mu(\Omega)$	$V(\Omega)$	$d(N_3H_9)$	x	$d(O_xH_9)$
Ip	0.357	−0.4874	0.194	32.78	1.014	5	2.806
IIIp	0.356	−0.4885	0.192	32.70	1.014	4	2.683
IIIn	0.364	−0.4855	0.188	31.64	1.014	4	2.531
IVp	0.363	−0.4852	0.194	32.37	1.010	5	3.521
IVn	0.373	−0.4782	0.190	30.88	1.015	5	2.412
Vp	0.362	−0.4857	0.195	32.52	1.010	4	3.389
Vn	0.366	−0.4832	0.190	31.40	1.014	4	2.426
VIp	0.362	−0.4849	0.191	32.51	1.014	5	2.781
VIIIp	0.368	−0.4830	0.192	32.19	1.009	5	3.500
VIIIn	0.384	−0.4728	0.185	29.68	1.015	5	2.322

[a] $q(\Omega)$ is the atomic charge, $E(\Omega)$ the total energy, $\mu(\Omega)$ the dipolar polarization, and $V(\Omega)$ the atomic volume. All of these values are in atomic units. Interatomic $d(N_3-H_9)$, $d(O-H_9)$ distances are in Å.

VIIp are omitted). Popelier's criteria e−h for conformers Ip, IIIp, IIIn, and VIp, for which these H-bonds have been assumed,[21−23] reveal no evidence even of interactions reminiscent of hydrogen bonding like those noticed above. However, Table 5 suggests some interaction between H_9 and O_5 atoms in rotamers IVn and VIIIn and between H_9 and O_4 atoms in IIIn and Vn. Increased charges, destabilized energies, decreased dipolar polarizations, and smaller atomic volumes with respect to their p counterparts are readily seen in these four conformers. This behavior agrees with the information provided by the interatomic distances: in fact, shorter O_4-H_9 (IIIn and Vn) and O_5-H_9 (IVn and VIIIn) distances are found in those rotamers. Note, however, that the O_5-H_9 distances are lower than the O_4-H_9 distances, which parallels the different magnitude of the changes in $q(\Omega)$, $E(\Omega)$, $\mu(\Omega)$, and $V(\Omega)$, larger in IVn and VIIIn than in IIIn and Vn. This could be understood in conventional terms by thinking that the hydroxyl oxygen is a worse hydrogen acceptor than the carbonyl oxygen. If the information in Tables 4 and 5 is considered together, rotamer IVn appears to be favored by interactions involving both hydrogens, H_6 and H_9. Note indeed that IVn is placed in the stability ordering in Table 2 immediately after IIp and IIn, the unique rotamers with a true intramolecular H-bond.

Potential Energies

With the aim to complement the study of intramolecular hydrogen bonding in the preceding section, we now discuss the competing effects leading to the stability of every rotamer in terms of the potential energy contributions of the molecular fragments NH_2, CH_2, CO, and OH. AIM theory allows us to obtain the different potential energy terms of an atom in a molecule, $V_T(\Omega) = V_{ne}(\Omega) + V_{ee}(\Omega) + V_{nn}(\Omega)$, computed for the basins Ω.[26,27] The sum over the atomic basins gives the corresponding quantity for the total system, $\Sigma_\Omega V_i(\Omega) = \langle V_i \rangle$, while partial sums can be used to obtain contributions from fragments NH_2, CH_2, CO, and OH. We list in Table 6 the nuclear−electron attraction terms V_{ne}, in Table 7 the total repulsion energy terms $V_{rep} = V_{ee} + V_{nn}$ (V_{ee} being the electron−electron repulsion and V_{nn} the nuclear−nuclear repulsions), and finally the total potential energies $V_T = V_{ne} + V_{rep}$ in Table 8. $L(\Omega)$ values for all of these energies are in the range of 5×10^{-3} to 2×10^{-5} for heavy atoms and in the range of 5×10^{-4} to 2×10^{-5} for hydrogens.

The differences from the minimum in every column of Table 6 for V_{ne} are plotted in Figure 7, where it is readily seen that these attractive energies vary dramatically along conformers for the fragments and the whole molecule as well. The amino group shows low ΔV_{ne} values in the structures for which topological evidence of intramolecular H-bonds was found (IIp, IIn, and VIIp), whereas the torsional changes in going from p to n rotamers in pairs IV, V, and VIII reduce this V_{ne}. Figure 7 reveals an opposite behavior of ΔV_{ne} in carbonyl and hydroxyl with huge oscillations for both groups. Conformers with $\psi = 0°$ (IIp, IIn, IIIp, IIIn, Vp, Vn, and VIIp) display systematically low ΔV_{ne} values for OH and high ΔV_{ne} values for CO, whereas the opposite effect is found in the rest of cases when $\psi = 180°$. Note the particularly low values for carbonyl in IVn and VIIIn,

TABLE 6: Nuclear−Electron Potential Energies V_{ne} for the NH_2, CH_2, CO, and OH Fragments and the Whole Molecule in Glycine Conformers[a]

conformer	NH_2	CH_2	CO	OH	total
Ip	−208.8914	−163.6356	−392.5239	−260.3431	−1025.3940
IIp	−211.2217	−164.1756	−388.1356	−264.7713	−1028.3042
IIn	−211.2656	−164.4050	−388.1530	−264.9918	−1028.8154
IIIp	−209.4454	−163.3494	−389.3453	−263.8411	−1025.9812
IIIn	−209.3673	−163.4279	−389.4349	−263.7752	−1026.0053
IVp	−208.5648	−163.8130	−391.4166	−260.2814	−1024.0758
IVn	−209.4885	−164.1385	−392.7781	−260.5347	−1026.9398
Vp	−209.2095	−163.7104	−389.0737	−263.3357	−1025.3293
Vn	−209.8852	−163.9732	−389.4132	−264.0469	−1027.2915
VIp	−208.8573	−164.3138	−392.0306	−259.8582	−1025.0599
VIIp	−210.1986	−163.3873	−388.5856	−263.5720	−1025.7435
VIIIp	−208.5671	−164.3864	−390.8703	−259.7609	−1023.5847
VIIIn	−209.5323	−164.7793	−392.3552	−260.1028	−1026.7696

[a] Computed with the MP2/6-311++G** electron density. Values are in atomic units.

TABLE 7: Repulsion Potential Energies $V_{rep} = V_{nn} + V_{ee}$, Sum of Electron−Electron Repulsion Energies V_{ee} plus Nuclear−Nuclear Repulsion Energies V_{nn}, for the NH_2, CH_2, CO, and OH Fragments and the Whole Molecule in Glycine Conformers[a]

conformer	NH_2	CH_2	CO	OH	total
Ip	96.8157	85.6517	166.7040	108.0238	457.1952
IIp	99.1052	86.1482	162.4270	112.4236	460.1040
IIn	99.1499	86.3645	162.4445	112.6537	460.6126
IIIp	97.3634	85.3742	163.5318	111.5150	457.7844
IIIn	97.2957	85.4434	163.6193	111.4503	457.8087
IVp	96.4773	85.8358	165.6115	107.9701	455.8947
IVn	97.4249	86.1145	167.0042	108.2139	458.7575
Vp	97.1199	85.7368	163.3018	110.9968	457.1553
Vn	97.8002	85.9421	163.6423	111.7191	459.1037
VIp	96.7929	86.2864	166.2317	107.5583	456.8693
VIIp	98.0717	85.4354	162.8220	111.2355	457.5646
VIIIp	96.4829	86.3722	165.0872	107.4697	455.4120
VIIIn	97.4771	86.7148	166.6079	107.7989	458.5987

[a] Computed with the MP2/6-311++G** electron density. Values are in atomic units.

TABLE 8: Total Potential Energies $V_T = V_{ne} + V_{rep}$ for the NH_2, CH_2, CO, and OH Fragments and the Whole Molecule in Glycine Conformers[a]

conformer	NH_2	CH_2	CO	OH	total
Ip	−112.0757	−77.9839	−225.8199	−152.3193	−568.1988
IIp	−112.1165	−78.0274	−225.7086	−152.3477	−568.2002
IIn	−112.1157	−78.0405	−225.7085	−152.3381	−568.2028
IIIp	−112.0820	−77.9752	−225.8135	−152.3261	−568.1968
IIIn	−112.0716	−77.9845	−225.8156	−152.3249	−568.1966
IVp	−112.0875	−77.9772	−225.8051	−152.3113	−568.1811
IVn	−112.0636	−78.0240	−225.7739	−152.3208	−568.1823
Vp	−112.0896	−77.9736	−225.7719	−152.3389	−568.1740
Vn	−112.0580	−78.0311	−225.7709	−152.3278	−568.1878
VIp	−112.0644	−78.0274	−225.7989	−152.2999	−568.1906
VIIp	−112.1269	−77.9519	−225.7636	−152.3365	−568.1789
VIIIp	−112.0842	−78.0142	−225.7831	−152.2912	−568.1727
VIIIn	−112.0552	−78.0645	−225.7473	−152.3039	−568.1709

[a] Computed with the MP2/6-311++G** electron density. Values are in atomic units.

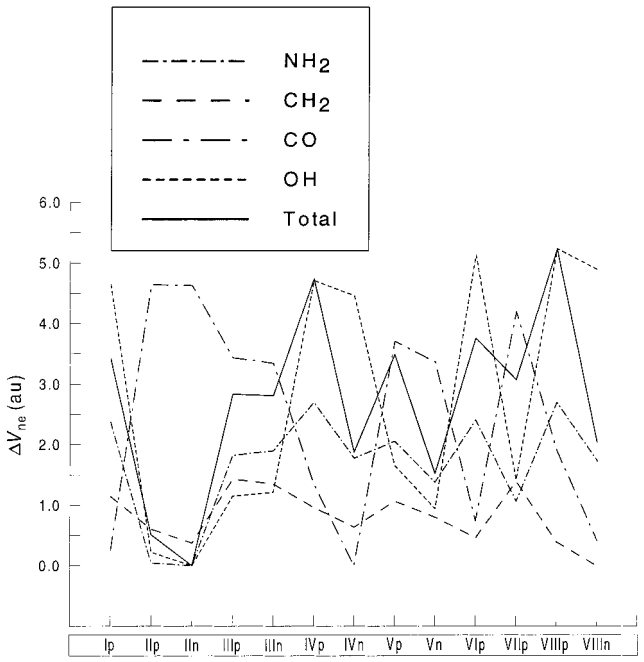

Figure 7. Differences with respect to the minimum in nuclear−electron potential energies for the molecular fragments NH_2, CH_2, CO, and OH and the whole molecule for the conformers of nonionized glycine.

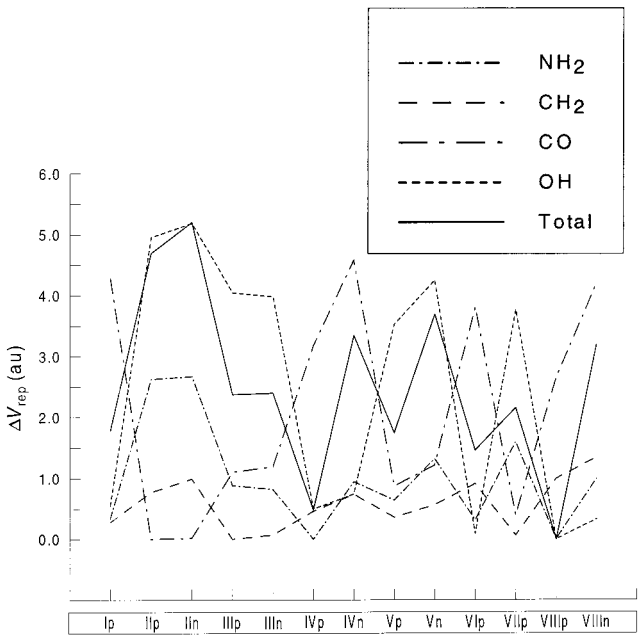

Figure 8. Differences with respect to the minimum in repulsion potential energies for the molecular fragments NH_2, CH_2, CO, and OH and the whole molecule for the conformers of nonionized glycine.

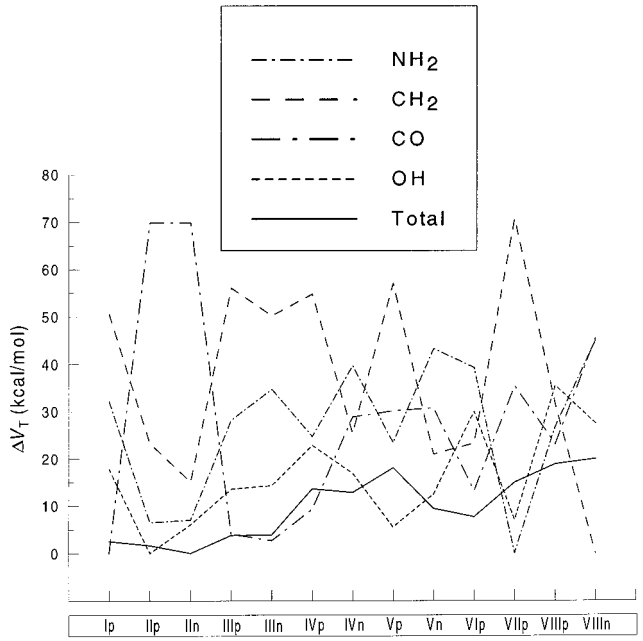

Figure 9. Differences with respect to the minimum in total potential energies for the molecular fragments NH_2, CH_2, CO, and OH and the whole molecule for the conformers of nonionized glycine.

for which an interaction involving O_5 was suggested in the preceding section. Finally, CH_2 displays less pronounced variations with a maximum relative change of 0.87%. Total attractive energies for the whole molecule resulting from fragment contributions also show large fluctuations. Conformers IIp and IIn display the two minimum values of total V_{ne} due to the especially low contributions of NH_2 and OH, as expected from the demonstrated existence of H-bonds in them. The following set of low total V_{ne} values is IVn, Vn, and VIIIn, three rotamers sharing the above suggested interaction involving H_9 related to the low ΔV_{ne} values of amino mainly responsible for those low total V_{ne}. The higher attraction energies are determined by the high ΔV_{ne} values of hydroxyl in IVp and VIIIp. Rotamers Ip, Vp, and VIp exhibit less unfavorable conformations with high V_{ne} mainly due to OH in Ip and VIp and CO in Vp. Finally, IIIp, IIIn, and VIIp present intermediate values resulting from a compromise between high V_{ne} for CO and low V_{ne} for OH. Except for the pair IIIp−IIIn, where the difference is nearly indistinguishable, a common feature of nonplanar arrangements is the significantly lower V_{ne} values for all of the molecular fragments.

The differences from every minimum for total repulsive energies listed in Table 7 are plotted in Figure 8. The variations in ΔV_{rep} along conformers are of the same order of magnitude as ΔV_{ne}, although the behavior displayed by both potential energies is just the opposite as far as conformations allowing low nuclear−electron attractions imply close proximity of groups and accordingly high repulsions among nuclei and electrons. Maxima in Figure 7 parallel thus minima in Figure 8, so that conformers most favored by the two lowest attractive energies, IIp and IIn, are disfavored by the highest total repulsive energies. However, although the attractions in amino and hydroxyl are equivalent in the pair IIp−IIn, the repulsions suffered by NH_2 are not as strong as those of OH, and consequently the repulsive destabilization in these conformers is due to hydroxyl, a reasonable result due to the different numbers of lone electron pairs in N and O atoms.

Table 8 lists total potential energies V_T for the molecular fragments and for the whole molecule; the differences from the minimum in every column, ΔV_T, are plotted in Figure 9. Note the scale in this figure: the maximum ΔV_T values for NH_2, CH_2, CO, and OH fragments are 45, 71, 70, and 35 kcal/mol, respectively, whereas the maximum ΔV_T for the whole molecule is 20 kcal/mol. The huge changes found in attraction and repulsion energies nearly cancel each other, leaving these small differences. Moreover, even the ΔV_T values for the fragments cancel to a great extent, yielding the subtle final changes in the molecular potential energy, which are next discussed.

The conformer of lowest potential energy is IIn (to which we assign $V_T = 0.0$ kcal/ mol), whereas its planar counterpart

IIp is the second stable conformer at 1.63 kcal/mol. The torsional change converting IIp into IIn yields a lower V_T in IIn as a balance between a global increase of 6.59 kcal/mol for NH_2, CO, and OH and a decrease of 8.22 kcal/mol for CH_2. The stability shared by IIp and IIn is to a great extent determined by NH_2 and OH groups (due in turn to their low V_{ne} energies) in agreement with the intramolecular H-bond found in them. The following conformer is Ip, with a relative V_T of 2.51 kcal/mol resulting from the low potential energies of OH and especially CO, which presents the minimum V_T for this fragment in Table 8. From Figures 7 and 8 the special stability of this rotamer, identified by all of the theoretical methods as the lowest lying, seems to be the consequence of low repulsions in CH_2, CO, and OH and low attractions in NH_2.

The pair of conformers IIIp−IIIn appears then at $V_T = 3.77$ and 3.89 kcal/mol, respectively. Their similar stabilities are brought about by a nearly complete cancellation between a high ΔV_T mainly due to large repulsions in NH_2 and OH and a low ΔV_T in CH_2 and CO produced by small repulsions and low attractions. It is difficult to predict any difference between IIIp and IIIn if they actually exist as separate structures. After a gap of ∼4 kcal/mol, VIp is found at $V_T = 7.66$ kcal/mol. The four molecular fragments display ΔV_T values in a narrow interval for this rotamer, the only one with all of the groups in antiperiplanar conformation ($\phi = 180°$, $\psi = 180°$, $\theta = 180°$) at which neither stabilizing nor destabilizing effects are evident.

The next structure in order of increasing potential energy is Vn at $V_T = 9.41$ kcal/mol. This conformer displays a high ΔV_T for amino and nearly identical ΔV_T values for the rest of the molecular fragments resulting from a similar cancellation of attractive and repulsive effects (see Figures 7 and 8). The marked decrease in the ΔV_T of CH_2 produced by the corresponding torsional change places Vn below its Vp counterpart. The following conformers are IVn and IVp with $V_T = 12.9$ and 13.6 kcal/mol, respectively. As noted before, IVp is the second conformer most disfavored by high attraction energies especially due to hydroxyl (see Figure 7), and although the low repulsion reduces to a great extent this effect, ΔV_T remains high for OH in IVp. All of these effects are inverted in IVn, leading to a net slight stabilization with respect to IVp mainly produced by the large decrease in ΔV_T for CH_2, in agreement with the synclinal conformation of CH_2 and NH_2 groups in IVn. The torsional movement in going from planar to nonplanar heavy-atoms geometries yields the stabilization of CH_2, noticeable in all of the pairs p−n.

The next conformer is VIIp at $V_T = 15.0$ kcal/mol. The topological evidence discussed above on a possible intramolecular H-bond with an internal instability agrees with the low potential energies of NH_2 and OH groups. It is, however, the high ΔV_T values of CO and especially CH_2 groups that make this rotamer so unstable. Inspecting its geometrical parameters,[33] one finds a C_1C_2 bond length longer and a $N_3C_2C_1$ bond angle significantly larger than those of the rest of the conformers. The instability in the five-membered ring seems to distort the CH_2 group, which in turn originates its anomalous high ΔV_T. Note how this instability makes VIIp much more unstable than IIp, the equivalent rotamer with $\psi = 0°$ and $\theta = 180°$. The next conformer, Vp, shows the same $\psi = 0°$, $\theta = 0°$ conformation as IIIp and IIIn, yet its V_T is 18.1 kcal/mol, well above the values of these rotamers. From the ΔV_T contributions of the molecular fragments in these three conformers, the distinctive feature in Vp is the larger instability of carbonyl due in turn to its high attraction energy. Inspecting the atomic contributions in CO, we found increases in the V_T of both atoms in Vp with respect to IIIp, but although this increase is small in O_5 (4 kcal/mol), it is 5 times larger in C_1 (22 kcal/mol). This agrees with the geometrical distortion suffered by carbonyl in Vp, large in C_1 and nearly unnoticeable in O_5. In fact, C_1O_5 bond lengths (1.2095 Å in IIIp and 1.2127 Å in Vp) and $O_4C_1O_5$ bond angles (123.12° in IIIp and 123.38° in Vp) are similar in both conformers, whereas the changes in C_1O_4 bond lengths (1.3559 Å in IIIp and 1.3451 Å in Vp) and $C_2C_1O_5$ bond angles (123.93° in IIIp and 122.06° in Vp) are larger.

Finally, the least stable conformers are VIIIp and VIIIn with $V_T = 18.9$ and 20.0 kcal/mol, respectively. The four molecular fragments in VIIIp present intermediate ΔV_T values in a very narrow rangel; the result of this situation is the lack of any stabilization factor in this rotamer. ΔV_T values of CO and NH_2 in VIIIn are even higher than in VIIIp as a consequence of their larger repulsions. Despite CH_2 stabilization due to the torsional change from VIIIp to VIIIn, this rotamer presents the highest V_T in Table 8. With regard to this special stability of CH_2, we have found in VIIIn effects the opposite of those mentioned above for VIIp: shorter C_1C_2 bond length and smaller $N_3C_2C_1$ angle.

Concluding Remarks

Thirteen conformers of nonionized glycine previously identified in ab initio calculations at the MP2/6-311++G** level of theory have been studied in terms of properties directly obtainable from the electron density. We have used the rigorous tools of AIM theory to analyze topologically the $\rho(\mathbf{r})$ and calculate the atomic contributions to nuclear−electron attraction and nuclear−nuclear and electron−electron repulsion potential energies. We have thus characterized the intramolecular interactions in the conformers by means of fundamental properties of the electron density itself. This analysis casts new light on the nature of the intramolecular effects in the set of rotamers, which constitutes the conformational PES of glycine and complements previous studies carried out in terms of qualitative empirical considerations common in chemistry. Because the glycine molecule is the simplest amino acid, this first study of intramolecular interactions in terms of the electron density may serve as a methodological reference for further studies on amino acid systems. The following general conclusions can be drawn from the present study.

Contrarily to previous assumptions, we found evidence of intramolecular hydrogen bonds in only two rotamers, IIp and IIn. A third conformer, VIIp, meets the requirements to form an intramolecular H-bond, but the topology reveals an internal stability that precludes its formation. Other interactions in which a hydrogen atom displays features reminiscent of H-bonds were found in some conformers. O−H···O interactions within carboxyl were identified in Ip, IIIp, IIIn, IVp, IVn, Vp, and Vn, whereas N−H···O interactions were found in IVn, VIIIn, and, to a lesser extent, Vn. The dominant effect of such interactions is the decrease of the nuclear−electron attraction energy of the groups involved. However, the opposite effect of both nuclear−nuclear and electron−electron repulsions cancels that stabilization to the extent of even raising the total potential energy of the groups in some conformers. Nevertheless, significantly lower total potential energies were found in IIp and IIn, in which the criteria posed by AIM theory to identify intramolecular H-bonds are fulfilled.

The cancellation between opposite attractive and repulsive effects leaves a final subtle balance of total potential energies with differences within 20 kcal/mol for the 13 conformers. Potential energy effects point to the pair IIp−IIn as the lowest

lying structures in agreement with the role played by their intramolecular H-bonds. The special stability of Ip due to a particularly favorable balance betwen opposite effects is here confirmed. After these three conformers, the pair IIIp−IIIn follows at 3.8 kcal/mol above the minimum. With regard to the higher energy rotamers, these effects confirm the instability of VIIp and the pair VIIIp−VIIIn, although the differences in their potential energies are much smaller than what could be expected from existing ab initio results. Although IVn, Vn, and VIIIn C_1 rotamers are clearly more stable than their planar C_s counterparts, the potential energy effects do not recognize any significant distinction between rotamers in pairs IIp−IIn and IIIp−IIIn.

Acknowledgment. We gratefully acknowledge financial support from the Dirección General de Enseñanza Superior e Investigación Científica, Project PB97-0268.

References and Notes

(1) (a) Jönsson, P. G.; Kvick, Å. *Acta Crystallogr., Sect. B* **1972**, *28*, 1827. (b) Power, L. F.; Turner, K. E.; Moore, F. H. *Acta Crystallogr., Sect. B* **1976**, *32*, 11.

(2) Albrecht, G.; Corey, R. B. *J. Am. Chem. Soc.* **1939**, *61*, 1087.

(3) Almlöf, J.; Kvick, Å.; Thomas, J. O. *J. Chem. Phys.* **1973**, *59*, 3901.

(4) Legros, J. P.; Kvick, Å. *Acta Crystallogr., Sect. B* **1980**, *36*, 3052.

(5) Destro, R.; Roversi, P.; Barzaghi, M.; Marsh, R. E. *J. Phys. Chem. A* **2000**, *104*, 1047.

(6) Ghazanfar, S. A. S.; Myers, D. V.; Edsall, J. T. *J. Am. Chem. Soc.* **1939**, *61*, 1087.

(7) (a) Machida, K.; Kagayama, A.; Saito, Y.; Kuroda, Y.; Uno, T. *Spectrochim. Acta* **1977**, *33A*, 569. (b) Kakihana, M.; Akiyama, M.; Nagumo, T.; Okamoto, M. Z. *Naturforsch.* **1988**, *43A*, 774.

(8) (a) Alper, J. S.; Dothe, H.; Lowe, M. A. *Chem. Phys.* **1992**, *161*, 199. (b) Jensen, J. H.; Gordon, M. S. *J. Am. Chem. Soc.* **1995**, *117*, 8159. (c) Ding, Y.; Krogh-Jespersen, K. *Chem. Phys. Lett.* **1992**, *199*, 261. (d) Ding, Y.; Krogh-Jespersen, K. *J. Comput.Chem.* **1996**, *17*, 338.

(9) Chakraborty, D.; Manogaran, S. *Chem. Phys. Lett.* **1998**, *294*, 56.

(10) Brown, R. D.; Godfrey, P. D.; Storey, J. W.; Bassez, M. P. *J. Chem. Soc., Chem. Commun.* **1978**, 547.

(11) (a) Suenram, R. D.; Lovas, F. J. *J. Mol. Spectrosc.* **1978**, *72*, 372. (b) Suenram, R. D.; Lovas, F. J. *J. Am. Chem. Soc.* **1980**, *102*, 7180.

(12) Ijima, K.; Tanaka, K.; Onuma, S. *J. Mol. Struct.* **1991**, *246*, 257.

(13) (a) Godfrey, P. D.; Brown, R. D. *J. Am. Chem. Soc.* **1995**, *117*, 2019. (b) Godfrey, P. D.; Brown, R. D.; Rodgers, F. M. *J. Mol. Struct.* **1996**, *376*, 65.

(14) Zheng, Y.; Neville, J. J.; Brion, C. E. *Science* **1995**, *270*, 786.

(15) Vishveshwara, S.; Pople, J. A. *J. Am. Chem. Soc.* **1977**, *99*, 2422.

(16) (a) Sellers, H. L.; Schäfer, L. *J. Am. Chem. Soc.* **1978**, *100*, 7728. (b) Schäfer, L.; Sellers, H. L.; Lovas, F. J.; Suenram, R. D. *J. Am. Chem. Soc.* **1980**, *102*, 6566.

(17) Dykstra, C. E.; Chiles, R. A.; Garrett, M. D. *J. Comput. Chem.* **1981**, *2*, 266.

(18) Jensen, J. H.; Gordon, M. S. *J. Am. Chem. Soc.* **1991**, *113*, 7917.

(19) (a) Ramek, M.; Cheng, V. K. W.; Frey, R. F.; Newton, S. Q.; Schäfer, L. *J. Mol. Struct. (THEOCHEM)* **1991**, *235*, 1. (b) Frey, R. F.; Coffin, J.; Newton, S. Q.; Ramek, M.; Cheng, V. K. W.; Momany, F. A.; Schäfer, L. *J. Am. Chem. Soc.* **1992**, *114*, 5369.

(20) Császár, A. G. *J. Am. Chem. Soc.* **1992**, *114*, 9568.

(21) Hu, C. H.; Shen, M.; Schaefer, H. F., III. *J. Am. Chem. Soc.* **1993**, *115*, 2923.

(22) Barone, V.; Adamo, C.; Lelj, F. *J. Chem. Phys.* **1995**, *102*, 364.

(23) Nguyen, D. T.; Scheiner, A. C.; Andzelm, J. W.; Sirois, S.; Salahub, D. R.; Hagler, A. T. *J. Comput. Chem.* **1997**, *13*, 1609.

(24) Gronert, S.; O'Hair, R. A. J. *J. Am. Chem. Soc.* **1995**, *117*, 2071.

(25) Coppens, P.; Abramov, Y.; Carducci, M.; Korjov, B.; Novozhilova, I.; Alhambra, C.; Pressprich, M. R. *J. Am. Chem. Soc.* **1999**, *121*, 2585.

(26) Bader, R. F. W. *Atoms in Molecules. A Quantum Theory*; Clarendon Press: Oxford, U.K., 1990.

(27) Popelier, P. *Atoms in Molecules. An Introduction*; Prentice Hall: Harlow, U.K., 2000.

(28) Becke, A. *J. Chem. Phys.* **1993**, *98*, 5648.

(29) (a) Koch, U.; Popelier, P. L. A. *J. Phys. Chem.* **1995**, *99*, 9747. (b) Popelier, P. L. A. *J. Phys. Chem. A* **1998**, *102*, 1873.

(30) Frisch, M. J.; Trucks, G. W.; Schlegel, H. B.; Scuseria, G. E.; Robb, M. A.; Cheeseman, J. R.; Zakrzewski, V. G.; Montgomery, J. A., Jr.; Stratmann, R. E.; Burant, J. C.; Dapprich, S.; Millam, J. M.; Daniels, A. D.; Kudin, K. N.; Strain, M. C.; Farkas, O.; Tomasi, J.; Barone, V.; Cossi, M.; Cammi, R.; Mennucci, B.; Pomelli, C.; Adamo, C.; Clifford, S.; Ochterski, J.; Petersson, G. A.; Ayala, P. Y.; Cui, Q.; Morokuma, K.; Malick, D. K.; Rabuck, A. D.; Raghavachari, K.; Foresman, J. B.; Cioslowski, J.; Ortiz, J. V.; Baboul, A. G.; Stefanov, B. B.; Liu, G.; Liashenko, A.; Piskorz, P.; Komaromi, I.; Gomperts, R.; Martin, R. L.; Fox, D. J.; Keith, T.; Al-Laham, M. A.; Peng, C. Y.; Nanayakkara, A.; Gonzalez, C.; Challacombe, M.; Gill, P. M. W.; Johnson, B.; Chen, W.; Wong, M. W.; Andres, J. L.; Head-Gordon, M.; Replogle, E. S.; Pople, J. A. *GAUSSIAN98*; Gaussian Inc.: Pittsburgh, PA, 1998.

(31) Biegler-Konig, F. W.; Bader, R. F. W.; Tang, T. *J. Comput. Chem.* **1982**, *13*, 317.

(32) Bader, R. F. W. *AIMPAC95 Program Package*; McMaster University: Hamilton, ON, Canada, 1998.

(33) We have found three mistakes in the geometrical parameters of glycine conformers (Table 3 of ref 20): the $C_2C_1O_5$ bond angle in IIn is 122.56° instead of 112.56°, the $H_7C_2C_1$ bond angle in VIIIn is 109.34° instead of 105.34°, and the $H_8C_2C_1$ bond angle in VIIIn is 105.70° instead of 109.70°.